HNO₃ Partitioning in Cirrus Clouds

S.K. Meilinger,^{1,2} A. Tsias,¹ V. Dreiling,³ M. Kuhn,⁴ Ch. Feigl,⁴ H. Ziereis,⁴ H. Schlager,⁴ J. Curtius,⁵ B. Sierau,⁵ F. Arnold,⁵ M. Zöger,⁶ C. Schiller,⁶ Th. Peter^{1,2}

Abstract. During the 1997 POLSTAR-1 winter campaign in northern Sweden a flight was performed across a cold trough of air ($\simeq 196$ K) in the tropopause region. Measurements of total water vapour, nitric acid, particles and reactive nitrogen (NO_y) were taken. The particle measurements indicate that about 3% of the particles in the moist tropospheric air were ice particles. Forward and backward facing NO_y inlets were used simultaneously to determine condensed phase HNO₃. The combined NO_y and particle measurements reveal that less than 1% of a monolayer of NO_v could have resided on the ice particles. This casts doubt on the hypothesis that sedimenting cirrus particles generally lead to a strong downward flux of NO_v. In addition to the NO_v measurements, independent HNO₃ measurements were used to determine total HNO₃. Although quantitative uncertainties do not allow to completely rule out that the NOy uptake on ice was limited by total HNO₃, the combined NO_y and HNO₃ data suggest that there was low uptake of NO_v on ice despite abundant HNO₃ in the gas phase. Model studies indicate, that the most likely explanation of the measured nitric acid partitioning is given by HNO₃ in ternary solution droplets coexisting with almost HNO₃ free ice in the same air mass.

Introduction

Lower stratospheric air is usually too dry to allow significant ice formation. Conversely, the upper troposphere is characterized by cold and moist air masses, hence providing an environment suitable for visible and sub-visible cirrus clouds. Ice particles may affect the composition of the atmosphere through both trace gas scavenging and heterogeneous surface reactions on cloud particles. However, little is known about HNO₃ uptake on ice under tropospheric conditions, where HNO₃ concentrations are much lower than in the stratosphere. In the troposphere the ice frostpoint ($T_{\rm ice}$) might be several degrees above the nitric acid trihydrate (NAT) equilibrium temperature ($T_{\rm NAT}$). Laboratory work shows that NAT nucleation on ice is unlikely at supersaturations $S_{\rm NAT} < 8$ [Worsnop et al., 1993] or 4-10 [Hanson, 1992]. However, HNO₃ is taken up as a thin supercooled liquid film [Zondlo

Copyright 1999 by the American Geophysical Union.

Paper number 1999GL900423. 0094-8276/99/1999GL900423\$05.00

et al., 1997] when temperatures fall below the HNO3-H2O dew point. This is corroborated by Koop [1996] who re-interpreted the decahydrate of Worsnop et al. [1993] as HNO3-H₂O liquid on ice, and similarly by Zondlo et al. [1997] reinterpreting a result of Hanson [1992]. Recent laboratory experiments by Abbatt [1997] and Zondlo et al. [1997] concerning HNO₃ uptake on ice above T_{NAT} suggest formation of about 0.1 and 1 monolayer HNO3 on ice, respectively. Model calculations by Lawrence and Crutzen [1998] based on a 0.1 monolayer uptake of HNO₃ suggest a very efficient vertical transport of HNO3 by sedimenting cirrus cloud particles which leads to changes of trace gases such as NOx and OH. In contrast, airborne measurements by Weinheimer et al. [1998] show less than 5% of a monolayer ice surface coverage. However, these authors argued that their finding might simply be due to a low total amount of HNO3, which was not measured.

Here we investigate HNO₃ partitioning in a cirrus cloud observed during POLSTAR-1. The measurements suggest that the maximum uptake of NO_y onto ice particles is less than 1% of a monolayer (1ML=10¹⁵molecules/cm²), even though the average total HNO₃ abundance was at least six times larger than the measured particle NO_y.

Ouasi-Lagrangian Measurements

During POLSTAR-1 the DLR Falcon performed an almost quasi-Lagrangian measurement on 24 January 1997, measuring total water, nitric acid, reactive nitrogen, trace gases (CO, O_3), differential particle densities and condensation nuclei. The flight followed approximately the direction of the horizontal wind, leading across a cold trough of air located northwest of Kiruna where a sub-visible cirrus cloud was encountered. The outward flight leg was performed at constant pressure (ca. 200 mb) cutting through a bundle of isentropes. The trace gas measurements clearly indicate when the aircraft crossed the tropopause. The stratospheric air encountered up- and downstream of the ice cloud was very dry with total water mixing ratios around $5\pm25\%$ ppmv H_2O . The moist tropospheric air inside the cloud contained up to $20\pm25\%$ ppmv H_2O [Schiller et al., this issue].

Results

Particle Spectra

From relatively dry and warm (205 K) stratospheric air the Falcon encountered a cold and rather moist troposphere with temperatures of 196 K, well below the ice frostpoint ($T_{\rm ice} \simeq 197-207$ K, depending on humidity). Figure 1 shows MASP differential number densities dn/dr and fitted log-normal distributions constrained by the CNC measurements at the small size limit. Inside the ice cloud the mea-

¹Max Planck Institute for Chemistry, Mainz.

² Atmospheric Sciences, ETH Zürich

³Institute for Atmospheric Physics, University of Mainz.

⁴Institute for Atmospheric Physics, DLR Oberpfaffenhofen.

⁵ Max Planck Institute for Nuclear Physics, Heidelberg

⁶Institute for Stratospheric Chemistry, KFA Jülich

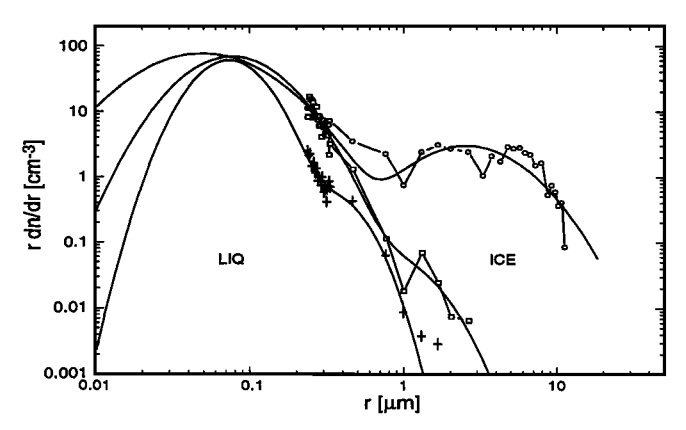


Figure 1. Tropospheric MASP particle spectra taken in the cloud (circles) and at the upwind edge of the cloud (squares) and one stratospheric spectrum downwind of the cloud (crosses). The spectra were averaged over 119, 175 and 500 sec respectively. Log-normal fits based on MASP and CNC data (smooth lines).

sured distributions may be fitted to log-normals with $n_{tot}^{\rm liq}=155.9/{\rm cm^3}$, $r_m^{\rm liq}=0.05\mu{\rm m}$, $\sigma^{\rm liq}=2.25$, $n_{tot}^{\rm ice}=5.26/{\rm cm^3}$, $r_m^{\rm ice}=2.56\mu{\rm m}$, $\sigma^{\rm ice}=2.01$. The instrumental uncertainty of MASP (due to Mie oscillations in the measured scattered light) is estimated as -30%/+200% in dn/dr and thus in surface area. That the total error is unlikely to be larger than a factor of two is supported by independent measurements of total H₂O [Schiller et al., this issue] of 20 ppmv. While the MASP particle volume corresponds to 15 ppmv, the remaining 5 ppmv in the gas phase match the ice vapor pressure at the relevant temperature. — In the region of the cirrus cloud about 3% of all particles contain ice (large particle mode in Fig. 1). While the details of the ice nucleation remain uncertain, it is conceivable that due to the stoichastic nature of the freezing process and the subsequent competitive growth only 3% of the particles froze. The smaller mode (Fig. 1) is interpreted as ternary droplets [Carslaw et al., 1994, Tabazadeh et al., 1994], from which we determined the H₂SO₄ loading of the atmosphere to be 0.2-1.9 ppbv (given by a maximum error of 15% in σ^{liq}), assuming thermodynamic equilibrium with the measured HNO₃ in the gas phase and water vapour over ice [Carslaw et al., 1995]. In the following we assume 0.6 ppbv H₂SO₄. Sensitivity studies (Table 1) suggest our results to be insensitive to this choice.

Uptake of NO_y on particles

Total reactive nitrogen (NO_y) was measured by an NO_y-detector with a forward and a backward pointing air intake. The difference between the NO_y channels in forward and backward direction (Δ NO_y=NO_y^{fwd}- NO_y^{bwd}) is a measure for the HNO₃ in particles larger than a certain radius r_0 (HNO₃^{ftcl>r₀}). As both channels have different sampling efficiencies, this difference has to be corrected by an overall enhancement factor E, where $E = \int_{r_0}^{\infty} dr (E_r/n^{>r_0}) (dn/dr)$. Here, $n^{>r_0}$ is the total number density for particles larger than the cut-off radius r_0 (below which both channels have comparable sampling efficiencies), and E_r is the enhancement factor for a particle with radius r as derived from wind-tunnel experiments. The overall enhancement factor depends strongly on r_0 (here $r_0 = 0.5 \mu$ m) and on the particle dis-

tribution. From particle measurements of dn/dr (Fig. 1) we determined the overall enhancement factor for the larger ice mode ($E^{\rm ice} \approx 90$) and for the liquid mode ($E^{\rm liq} \approx 20$). Using these enhancement factors, we find

$$\text{HNO}_3^{\text{ptcl}>r_0} = \alpha \Delta \text{NO}_y / E^{\text{ice}} + (1 - \alpha) \Delta \text{NO}_y / E^{\text{liq}}$$
 (1)

where α is the fraction of HNO₃^{ptcl>r₀} sitting on ice and $(1-\alpha)$ the fraction sitting in droplets.

Due to the error in dn/dr we estimate the uncertainty in E as -30%/+200%. However as E is limited by $E_{max}=140$ (ratio of the ambient flow velocity relative to the aircraft and the velocity in the sample probe) the error for $E^{\rm ice}$ is reduced to -30%/+60%. Considering the sensitivity of the NO_y detector and the error in E, we estimate the uncertainty of HNO₂^{ptcl>r₀} as \pm 80% (independent of α).

Figure 2a shows $\text{HNO}_3^{\text{ice}}|_{max} \equiv \text{HNO}_3^{\text{ptcl}}|_{\alpha=1} = \Delta \text{NO}_y/E^{\text{ice}}$, assuming that all particulate ΔNO_y resides on ice. To compare our results with 1 and 0.1 ML uptake (corresponding to findings by Zondlo et al. [1997] and Abbatt [1997]) we multiplied the surface area of the cloud (419 $\mu\text{m}^2/\text{cm}^3$) derived from the ice mode in Fig. 1 with the corresponding surface coverages and converted to mixing ratio (using 1ML=10¹⁵/cm²). Obviously HNO $_3^{\text{ice}}|_{max}$ (2-8 pptv) is lower than 0.01 ML, a conclusion directly derived from the measurements.

Partitioning of HNO₃

The question arises whether the 0.01 ML is caused by a limited availability of nitric acid. Gaseous nitric acid (HNO3MS) was measured using an ion-molecule-reaction mass-spectrometer (IMRMS), which has a forward facing air intake [Schneider et al., 1998]. Possibly some evaporation of HNO3-containing particles occurs during the residence time (50 ms) in the sampling line of the HNO₃ detector. The enhancement factor E^* for IMRMS particle oversampling is at most $E_{max}^* = 4.5$ for large ice particles, while it is about 1 for smaller liquid particles. Hence, total nitric acid is limited by $\text{HNO}_3^{\text{MS}}/E^* \leq \text{HNO}_3^{\text{tot}} \leq \text{HNO}_3^{\text{MS}} + \text{HNO}_3^{\text{ptcl}}$ depending on the degree of evaporation. The error for HNO $^{MS}_{3}$ is $\pm 80\%$ (due to uncertainties in rate coefficient, background, reaction time, mass discrimination and ion evolution; see Feigl et al. [this issue] for further details).

Inspection of IMRMS yields the upper and lower limits of HNO₃^{tot} shown in Fig. 2a (diamonds). The lower limit is about 25 pptv (if HNO₃^{tot}=HNO₃^{MS}/ E^* with $E^*=4.5$) which is still on average six times larger than HNO₃^{ice}|_{max}. In this case, the error bars for HNO₃^{ice}|_{max} and HNO₃^{tot} are sightly overlapping. Hence it cannot be completely excluded that all HNO₃ is deposited on ice and the small amount (< 0.01 ML) is limited by availability of HNO₃. If so, this would imply that the total HNO₃ was only around 5-8 pptv and that

Table 1. HNO₃ uptake in liquid and ice particles assuming a thin ternary solution layer on the ice. Sensitivity studies for varying H_2SO_4 due to uncertainties in σ^{liq} .

σ_{liq}	H ₂ SO ₄ ppbv	HNO101	HNO tot	HNO3ce HNO3ct	[ML]
2.0	0.25	13%	86%	0.6%	0.2%
2.25	0.6	29%	70%	1.3%	0.4%
2.45	1.2	58%	39%	2.6%	0.9%

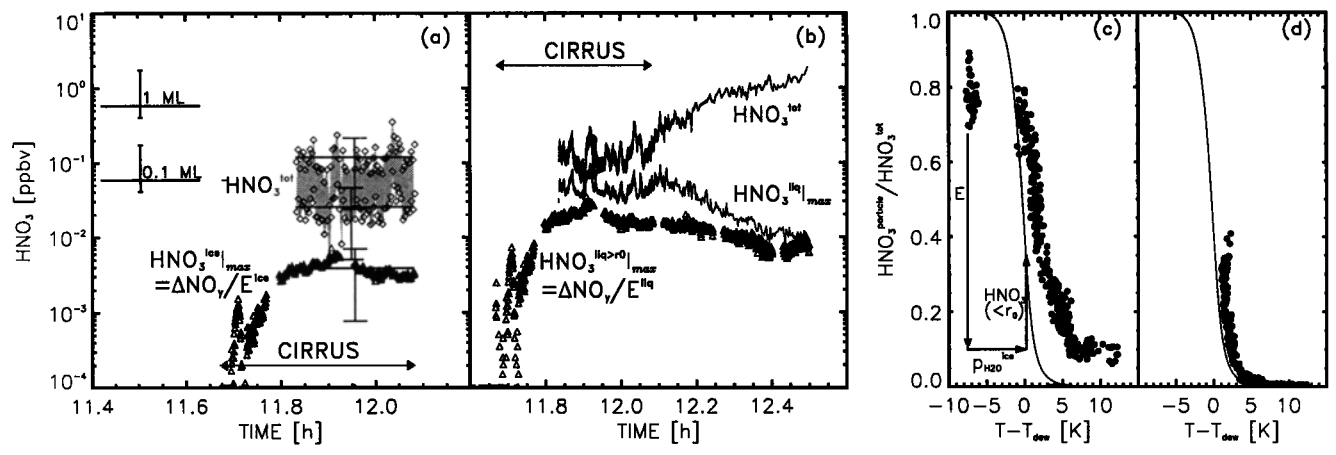


Figure 2. Left: Measured HNO₃^{tot} and uptake of NO_y into particles corrected for enhancement assuming a cut-off radius $r_0=0.5\mu\mathrm{m}$. (a) HNO₃^{ice}| $_{max}=\Delta\mathrm{NO_y}/E^\mathrm{ice}$ with $E^\mathrm{ice}=90$ (triangles) assuming measured $\Delta\mathrm{NO_y}$ to reside on ice (larger mode in Fig. 1). Upper and lower limits (diamonds) of HNO₃^{tot} (shaded area) given by HNO₃^{MS}+ HNO₃^{ice}| $_{max}$ assuming the mass spectrometer to measure only gas phase HNO₃, and by HNO₃^{MS}/ E^* assuming the particles to evaporate and enhance the MS signal (with $E^*=4.5$), respectively. 1 ML and 0.1 ML uptake on the ice surface in Fig. 1. (b) HNO₃^{liq}| $_{max}=\Delta\mathrm{NO_y}/E^\mathrm{liq}$ with $E^\mathrm{liq}=20$ (triangles) assuming measured $\Delta\mathrm{NO_y}$ to reside in droplets (small mode in Fig. 1). HNO₃^{tot} (upper shaded area) and HNO₃^{liq}| $_{max}=\mathrm{HNO_3}^\mathrm{liq}>^\mathrm{r0}$ | $_{max}+\mathrm{HNO_3}^\mathrm{liq}<^\mathrm{r0}$ (lower shaded area) with HNO₃^{liq}| $_{max}$. Lower and upper limits of shaded areas are given by HNO₃^{tot}= HNO₃^{MS}/ E^* (with $E^*=1$) and HNO₃^{MS}+HNO₃^{liq}| $_{max}$, respectively. The black dots indicate data used for comparison with model calculations in Fig. 3. Right: Measured HNO₃ uptake into liquid particles as a function of $T-T_\mathrm{dew}$. (c) Raw data $\Delta\mathrm{NO_y}/(\mathrm{HNO_3}^\mathrm{MS}+\Delta\mathrm{NO_y})$, (d) data corrected for enhancements ($E=E^\mathrm{liq}$) and cut-offs (HNO₃^{liq<ro>r0}) assuming the IMRMS measures gas phase only (HNO₃^{liq}| $_{max}/(\mathrm{HNO_3}^\mathrm{MS}+\mathrm{HNO_3}^\mathrm{liq}|_{max})$ For data below T_ice we additionally corrected for the decrease of the HNO₃-H₂O dew point (several K) due to H₂O depletion after ice particle formation (p_{120}^liq). Theoretical curve: liquid HNO₃-H₂SO₄-H₂O solution with 0.6 ppbv H₂SO₄ (from Fig. 1).

depletion of HNO₃ had occurred in the air mass prior to the measurement [Feigl et al., this issue]. However, it seems to be more likely that HNO₃^{tot} was significantly larger than HNO₃^{ice}|_{max}, and therefore the question arises, why the available nitric acid was not taken up by the ice particles. This is hardly due to diffusive limitation, as the time constant $\tau = (4\pi r_m n_{tot} D_g \exp(\ln^2 \sigma/2))^{-1}$ for diffusive transport of HNO₃ (with gas diffusion constant D_g) to a particle distribution (as in Fig. 1) is on the order of a few minutes.

If the measured ΔNO_y did not reside on ice particles but in the ternary HNO₃-H₂SO₄-H₂O droplets (HNO₃^{liq>r0} $|_{max}$ $HNO_3^{ptcl>r_0}|_{\alpha=0} = \Delta NO_y/E^{liq}$) one obtains the scenario plotted in Fig. 2b. To consider that only droplets larger r_0 are measured, but smaller droplets contain HNO3 as well, we calculate $\text{HNO}_3^{\text{liq}}|_{max} = \text{HNO}_3^{\text{liq} > \text{r0}}|_{max} + \text{HNO}_3^{\text{liq} < \text{r0}}$ using $\text{HNO}_3^{\text{liq} < \text{r0}}/\text{HNO}_3^{\text{liq,theor}} = V^{\text{liq} < \text{r0}}/V^{\text{liq}}$, where the volumes and the thermodynamic function HNO₃^{liq,theor} are obtained from an equilibrium ternary solution model [Carslaw et al., In this calculation we use HNO₃^{gas} = HNO₃^{tot} - $HNO_3^{liq}|_{max}$, particle number densities, distribution width and sulfate loading from MASP and CNC. In the cirrus we assume $p_{\text{H}_2\text{O}}^{\text{gas}} = p_{\text{H}_2\text{O}}^{\text{ice}}$. Again, thermodynamic equilibrium is a valid assumption (as the particle number density is high leading to $\tau \simeq 4$ min). Finally, HNO₃^{tot}=HNO₃^{MS}/ E^* with $E^* = 1$ or $HNO_3^{tot} = HNO_3^{MS} + HNO_3^{liq}|_{max}$ depending on the unknown degree of evaporation in IMRMS, which explains the shaded areas in Fig. 2b.

From $\text{HNO}_3^{\text{liq}}|_{max}$ and $\text{HNO}_3^{\text{tot}}$ in Fig. 2b the degree of consistency between the observed and the ternary thermodynamic HNO_3 can be tested. Assuming ternary droplets and HNO_3 -free ice particles ($\alpha=0$), Figs. 2c,d show the ratio $\text{HNO}_3^{\text{liq}}|_{max}$ / $\text{HNO}_3^{\text{tot}}$ as a function of $T-T_{\text{dew}}$ ($T_{\text{dew}}=\text{HNO}_3$ -H₂O dew point [Carslaw et al., 1995]) before (2c) and after (2d) correcting for enhancements (E), cut-offs (HNO $_3^{\text{liq}}<^{\text{ro}}$) and the decrease of the HNO₃-H₂O dew point by several Kelvin due to ice-induced depletion of H₂O from the gas phase ($p_{\text{H}_2\text{O}}^{\text{ice}}$). This representation accounts for differences in total water and total HNO₃ in different air masses and extracts the partitioning of HNO₃ between the gas and particles. It can be seen that the observed HNO₃ uptake is in fairly good agreement with the expected HNO₃ content of ternary HNO₃-H₂SO₄-H₂O droplets.

Trajectory Modeling and Discussion

A spectral microphysical box model calculation [Meilinger et al., 1995; Tsias et al., 1997] was used to describe the evolution of a droplet distribution due to diffusive uptake of $\rm H_2O$ and $\rm HNO_3$ by liquid and ice particles along an isentropic trajectory ending at the flight path (from ECMWF, corrected for $\simeq 5$ K temperature offset according to measured T). For these calculations we assumed that 3% of the droplets freeze as water ice at $T_{\rm ice}$ -3 K, and that NAT can only nucleate if ice is already present and if $S_{\rm NAT} > 8$. Calculations in Figure 3 refer to conditions encountered in the ice cloud (Fig. 1) with

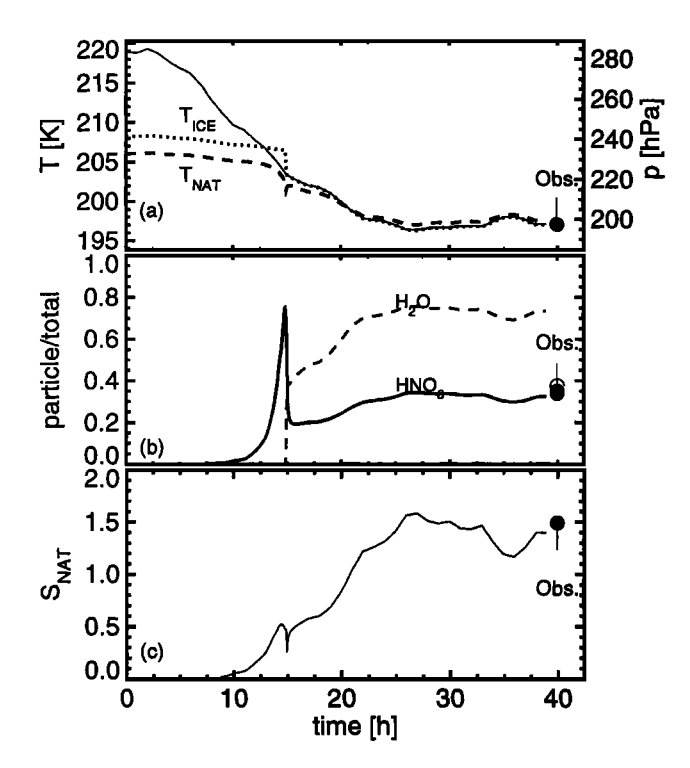


Figure 3. Particle growth of a droplet distribution (Fig. 1) due to diffusive uptake of H_2O and HNO_3 by liquid and ice particles along an isentropic trajectory. Calculations for 20 ppmv atmospheric water content and 0.2 ppbv HNO_3 assuming 3% ice particle formation 3 K below the frostpoint. The black dots correspond to the data points indicated in Fig. 2b. (a) Temperature and pressure history. (b) Partitioning of HNO_3 (solid line) and H_2O (dashed line) between gas phase and particles; solid dot: ternary liquid film on ice, α =4.3% (see Tab. 1); open dot: no HNO_3 on ice, α =0. (c) Supersaturation with respect to NAT.

20 ppmv H₂O, 0.6 ppbv H₂SO₄ and 0.2 ppbv HNO₃. Before ice particle formation, about 80% of the HNO3 is accommodated in the ternary droplets (Fig. 3b). Nevertheless, these droplets consist mainly of H₂O and H₂SO₄ with less than 5 wt% HNO3. When ice forms, HNO3 degasses from the droplets due to H₂O depletion. Monolayer uptake of HNO₃ onto ice would completely deplete the gas phase in contrast to observational evidence. Also, NAT is unlikely to nucleate on the ice particles due to the small supersaturations (Fig. 3c). Supercooled binary HNO₃-H₂O solutions on ice surfaces [Zondlo et al., 1997] can be excluded, as they cannot coexist with ternary solution droplets and would readily evaporate. However, if we assume HNO3 and H2SO4 to be expelled from the ice during droplet freezing, a thin ternary liquid layer could exist in equilibrium on the ice surface. Under such conditions the ice particles carry about 1% of the total HNO₃ (corresponding to 0.4% ML, see Table 1) and the remaining droplets about 30% (corresponding to about 2 wt%). In quantitative terms this leads to a small improvement of the agreement between measured and expected droplet uptake compared to HNO3-free ice (see difference between open and solid dot in Fig. 3b). More importantly, in qualitative terms such a ternary liquid coating of ice would explain the difference compared to the latoratory measurements, in which no H₂SO₄ was present. An alternative explanation could be Langmuir-like adsorption of HNO₃ on ice, which might represent a very small HNO₃ uptake due to the lower HNO₃ partial pressures in the cloud ($\leq 4 \times 10^{-8}$ mb at 196 K) compared to the laboratory experiments (except 1 datapoint by Zondlo et al., [1997]). In the absense of conclusive experimental evidence, it cannot be excluded that the surface coverage is less than 1% of a ML at such low partial pressure. No matter what the precise uptake mechanism of the small HNO₃ uptake on ice is, the present case suggests that most of the HNO₃ resides in the droplets and the gas phase.

Acknowledgments. We thank R. Alfier and E. Reimer for trajectory calculations. This project was in part supported by BMBF under several contracts.

References

Abbatt, J.P.D., Interaction of HNO₃ with water-ice surfaces at temperatures of the free troposphere, *Geophys. Res. Lett.*, 12, 1479-1482, 1997.

Carslaw, K.S., et al., Stratospheric aerosol growth and HNO₃ gas phase depletion from coupled HNO₃ and water uptake by liquid particles Geophys. Res. Lett., 21, 2479-2482, 1994.

Carslaw, K.S., et al., An analytic expression for the composition of aqueous HNO₃-H₂SO₄ stratospheric aerosols, Geophys. Res. Lett., 22, 1877-1880, 1995.

Feigl, Ch., et al., Observation of NO_y uptake by particles in the Arctic tropopause region at low temperature, this issue.

Hanson, D., The uptake of HNO₃ onto ice, NAT and frozen sulfuric acid, Geophys. Res. Lett., 19, 2063-2066, 1992.

Hanson, D. and K. Mauersberger, Laboratory studies of the nitric acid trihydrate: Implications for the South polar stratosphere, Geophys. Res. Lett., 15, 855-858, 1988.

Koop, Th., Die Bildungsmechanismen von Polaren Stratosphärenwolken, Dissertation (PhD), Mainz University, 1996.

Lawrence, M.G. and P.J. Crutzen, The impact of cloud particle gravitational settling on soluble trace gas distributions *Tellus*, 50B, 263-289, 1998 Meilinger, S.K., et al., Size-dependent stratospheric droplet composition in the composition of the composition

lee wave temperature fluctuations, Geophys. Res. Lett., 22, 3031-3034, 1995

Schneider, J., et al., The temporal evolution of the ratio HNO₃/NO_y in the arctic lower stratosphere from January to March 1997, Geophys. Res. Lett., submitted, 1998

Schiller, C., et al., Ice particle formation and sedimentation in the tropopause region: A case study based on in-situ measurements of total water during POLSTAR 1997, this issue.

Tabazadeh, A., et al., A study of Type I polar stratospheric cloud formation, Geophys. Res. Lett., 21, 1619-1622, 1994

Tsias, A., et al., Freezing of polar stratospheric clouds in orographically induced warming events, Geophys. Res. Lett., 18, 2303-2306, 1997

Weinheimer A.J., et al., Uptake of NO_y on wave cloud particles Geophys. Res. Lett., 25, 1725-1728, 1998.

Worsnop D.R., et al., Vapor pressures of solid hydrates of nitric acid, Science, 259, 71-74, 1993.

Zondlo, M.A., et al., Uptake of HNO₃ on ice under upper tropospheric conditions, Geophys. Res. Lett., 24, 1391-1394, 1997.

S.K. Meilinger, A. Tsias, Max Planck Institut für Chemie, Postfach 3060, 55020 Mainz, Germany

V.Dreiling, Institut für Physik der Atmosphäre, Johannes Gutenberg University Mainz, Becherweg 21, 55020 Mainz, Germany.

Ch. Feigl, M. Kuhn, H. Schlager, H. Ziereis, Institut für Physik der Atmosphäre, Deutsche Forschungsanstalt für Luft- und Raumfahrt e.V., 82230 Wessling, Germany.

F. Arnold, J. Curtius, B. Sierau, Max Planck Institut für Kernphysik, Postfach 103980, 69029 Heidelberg, Germany.

C. Schiller, M. Zöger, ICG-1, Institut für stratosphärische Chemie Forschungszentrum Jülich, KFA, Postfach 1913, 52405 Jülich, Germany.

Th. Peter, Atmospheric Sciences, Hönggerberg HPP, 8093 Zürich, Switzerland.

(Received December 28, 1998; revised May 7, 1999; accepted May 10, 1999.)